Advantage of new ventilation method for cardiopulmonary resuscitation qualitatively captured by simple respiratory mechanics models

Pigot, Harry; Sancho, Carlos B.; Paskevicius, Audrius; Steen, Stig; Soltesz, Kristian

Published in:
2020 American Control Conference (ACC)

DOI:
10.23919/ACC45564.2020.9147868

2020

Document Version:
Peer reviewed version (aka post-print)

Advantage of new ventilation method for cardiopulmonary resuscitation qualitatively captured by simple respiratory mechanics models

Henry Pigot[1], Carlos B. Sancho[2], Audrius Paskevicius[3], Stig Steen[3], Kristian Soltesz[1]

***Abstract*— First responders to cardiac arrest depend on cardiopulmonary resuscitation to keep patients alive. A new ventilation method, phase-controlled intermittent insufflation of oxygen, was previously shown to improve heart perfusion during cardiopulmonary resuscitation in a large-animal study, outperforming the best currently known ventilation method. This paper investigates whether the advantage of the new method can be explained using standard linear lumped-parameter models of respiratory mechanics. The simple models were able to qualitatively capture the improvement.**

I. Introduction

Cardiopulmonary resuscitation (CPR) is the standard first response to cardiac arrest. It combines two elements to circulate oxygenated blood through the body: chest compressions and gas exchange in the lungs. The objective during compression is to eject blood from the heart by raising the pressure in the heart above systemic blood pressure. The heart itself is perfused through the coronary arteries during chest decompression [1]. Coronary perfusion is driven by the pressure difference between the aorta and the right atrium — the coronary perfusion pressure (CPP) — as illustrated in Fig. 1. CPP is the best known hemodynamic indicator that an arrested heart will resume beating as a result of CPR treatment [2].

The heart and lungs are located inside the thorax, shown in Fig. 2. The pressure in the thorax (P_{thorax}) is a key component of blood transport in and out of the heart during CPR [3]. P_{thorax} changes the pressure surrounding the heart, pushing blood out of the aorta and pulmonary artery or allowing blood to flow back in from the pulmonary veins and vena cava. Flow opposite the normal direction of circulation is prevented by venous and heart valves or vein collapse [4]. Increasing P_{thorax} in the compression phase increases the ventricular pressures to facilitate blood ejection. Decreasing P_{thorax} in the decompression phase lowers the right atrial pressure, resulting in a higher CPP.

Intratracheal pressure, measured in the airway near the lungs, is closely coupled to P_{thorax} and can be measured with less clinical invasion than thoracic pressure. As such, it is used as an experimental indicator of P_{thorax}. While lung volume is being manipulated by oxygen insufflation, intratracheal pressure should be kept below 50 cmH_2O to avoid damaging the lungs [5].

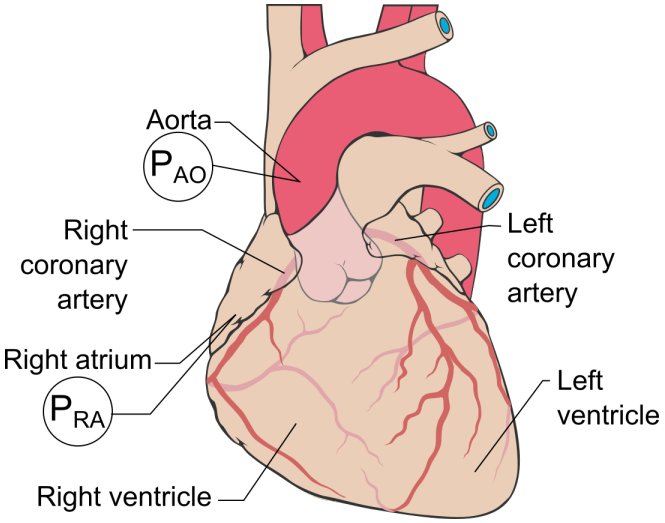

Fig. 1: Coronary perfusion flows across the pressure gradient between the aorta (P_{AO}) and right atrium (P_{RA}). Coronary perfusion pressure is the difference between P_{AO} and P_{RA}.[4]

Active compression-decompression mechanical CPR (mCPR) is performed by a machine, providing a precise compression depth and frequency. mCPR lowers P_{thorax} during decompression by actively pulling the thorax back to its original volume using a suction cup attached to the sternum [1], [6]. Combining mCPR with continuous insufflation of oxygen (CIO) results in a higher CPP compared to standard ventilation methods [7]. During CIO, oxygen is insufflated through a special endotracheal tube shown in Fig. 3. It enables oxygen delivery to the lungs without obstructing ventilation.

Chest compression and oxygen insufflation can be used as independent control signals to maximize P_{thorax} variations within safe limits, as illustrated in Fig. 2. The dynamics of the lungs and thorax have a low-pass effect on changes in lung volume due to oxygen insufflation. Phase-controlled intermittent insufflation of oxygen (PIIO), introduced in [8] and defined in Fig. 4, was suggested as a means to account for these dynamics. During PIIO, oxygen insufflation is turned off prior to active decompression, allowing the lung volume and P_{thorax} to decrease. Oxygen insufflation is resumed prior to the compression phase, increasing the lung volume and P_{thorax}. PIIO and CIO use the same type of endotracheal tube for oxygen insufflation. A preclinical study

[1]Department of Automatic Control, Lund University, P.O. Box 118, SE 221-00, Lund, Sweden henry.pigot@control.lth.se, kristian.soltesz@control.lth.se

[2]Departamento de Ingenieria de Sistemas y Automatica, Universitat Politecnica de Valencia, Camino de Vera s/n, 46022 Valencia, Spain carbasa3@doctor.upv.es

[3] Department of Cardiothoracic Surgery, Lund University and Skåne University Hospital, SE 221-85, Lund, Sweden

[4]Image modified from Patrick J. Lynch, "Coronary.pdf", wikimedia.org, CC BY-SA 3.0.

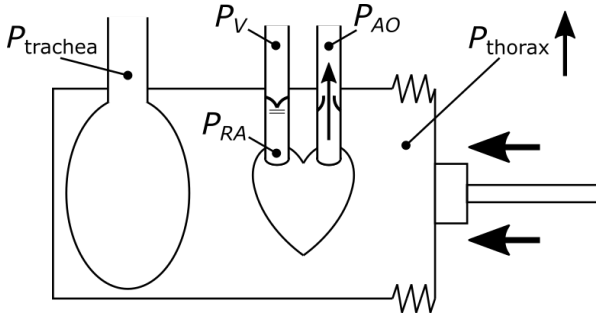

(a) Compression

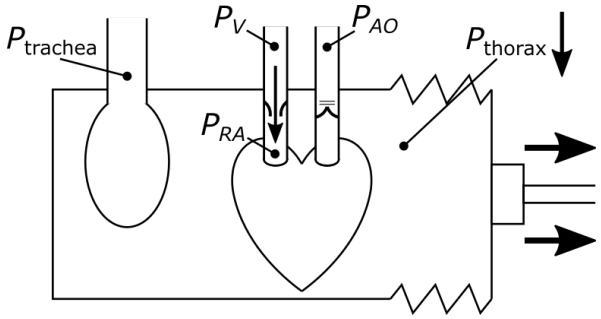

(b) Decompression

Fig. 2: The lungs (left), and heart with vessels entering/exiting the thorax (right) are shown in a box representing the thorax. The arrows on the right indicate chest compression or decompression. (a) shows the compression phase during which P_{thorax} can be maximized by lowering the volume of the thorax and increasing the volume of the lungs. P_{thorax} squeezes the heart such that the left ventricular pressure exceeds the aortic pressure P_{AO}. Blood flows across the gradient through the aortic valve. Retrograde flow from the right atrium is prevented by venous valves or vein collapse. (b) shows the decompression phase where P_{thorax} can be minimized by increasing the volume of the thorax and decreasing the volume of the lungs. P_{thorax} drops, pulling the right atrial pressure P_{RA} below venus pressure P_V. Blood flows across this pressure gradient filling the right atrium, while retrograde flow through the aorta is prevented by the aortic valve. Intratracheal pressure is shown as P_{trachea}.

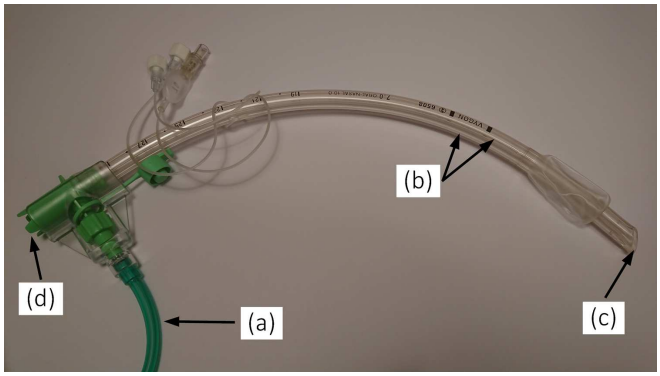

Fig. 3: A Boussignac endotracheal tube for cardiac arrest (VYGON, Ecouen, France). Oxygen is supplied through the green tube (a), whereafter it flows through narrow channels in the wall of the tube (b) and exits at the tip. The main lumen is open at both ends (c) and (d), allowing constant ventilation of gas from the lungs.

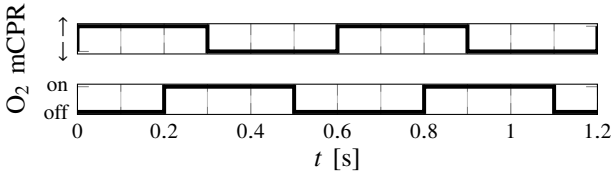

Fig. 4: Two full compression cycles with the PIIO ventilation method: phase shifted synchronization between the chest compression device (mCPR) state and oxygen insufflation (O_2). Figure reused with permission from [8].

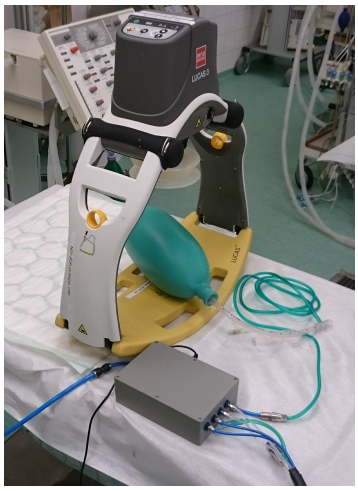

Fig. 5: An mCPR device and the controller (gray box) used to coordinate mCPR and oxygen insufflation during PIIO, with a balloon representing the lungs.

has shown that PIIO results in higher CPP and compression phase aortic pressure than CIO [8]. The electronic controller developed for coordinating PIIO is shown in Fig. 5 together with an mCPR device.

Here we investigate whether the advantage of PIIO in comparison to CIO can be qualitatively explained using simple lumped-parameter models of respiratory mechanics from literature. Two of the common circuit models of respiratory mechanics were modified to simulate intratracheal pressure dynamics during PIIO and CIO. This work is an analysis of the outcomes of those initial simulations, their limitations, and how they compare to the outcomes of the preclinical study. The circuit models take advantage of the direct analogy between the equations governing electric circuits and fluid systems [9], [10]. The analogous parameters are shown in Table I. The method is divided into two parts: the first describes the two models used for simulation of the ventilation methods and the second describes the preclinical study that the simulation results are compared to.

II. Method

A. Simulation

Respiratory mechanics can be modelled by a resistor, inductor, and capacitor (RIC) in series shown in Fig. 6 [9], [11]. The resistor and inductor represent the flow resistance and inertance of the airway, respectively, while the capacitor

TABLE I: Analogy between electrical and fluidic systems

Electrical System		Fluidic System	
Parameter	Unit	Unit	Parameter
Current	A	L/s	Flow
Voltage	V	cmH_2O	Pressure
Charge	C	L	Volume
Resistance	Ω	$cmH_2O/(L/s)$	Flow resistance
Capacitance	F	L/cmH_2O	Compliance
Inductance	H	$cmH_2O/(L/s^2)$	Inertance

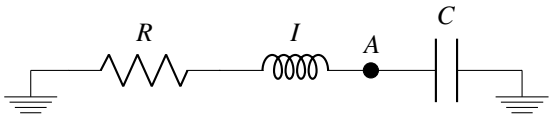

Fig. 6: The RIC model of respiratory mechanics. Ground potential corresponds to atmospheric pressure. R is the resistance of the airway. I is the inertance of the airway. C is the compliance of the lungs. The voltage between point A and ground represents intratracheal pressure.

TABLE II: Component values and descriptions for the RIC model of respiratory mechanics.

Component	Value	Description
R	2.76 Ω	Central airway resistance
I	6.39 mH	Airway inertance
C	11.7 mF	Lung compliance

TABLE III: Component values and descriptions for the Mead model of respiratory mechanics.

Component	Value	Description
R_C	3.26 Ω	Central airway resistance
I	14.5 mH	Airway inertance
C_L	1.12 kF	Lung compliance
R_P	1.66 Ω	Peripheral airway resistance
C_B	7.69 mF	Main bronchi compliance
C_W	47.6 mF	Chest wall compliance
C_E	0.32 mF	Extrathoracic compliance

represents the compliance of the lungs. Intratracheal pressure is given by the voltage between point A and ground potential.

The Mead model, shown in Fig. 7, expands the RIC model to separately account for the dynamics of the bronchi, alveoli, chest wall, and compliances outside the thorax [10], [11]. The components are described in Table III. As in the RIC model, intratracheal pressure is given by the voltage between point A and ground potential.

Component values identified from healthy volunteers have been used here for the RIC [12] and Mead [13] models, given in Table II and III, respectively. The values were obtained by minimizing the impedance error by the least squares method in comparison to data acquired through impulse oscillometry.

In CPR, chest compressions and oxygen insufflation are amplitude limited signals. Compressions are limited by the physiology of the thorax and oxygen insufflation is limited by the safe bounds on pressure within the lungs. Waveforms as close to a square wave as practical were chosen to maximize the energy delivered within those amplitude constraints. This follows directly from the definition of the $\mathcal{L}_2$-norm, representing signal energy.

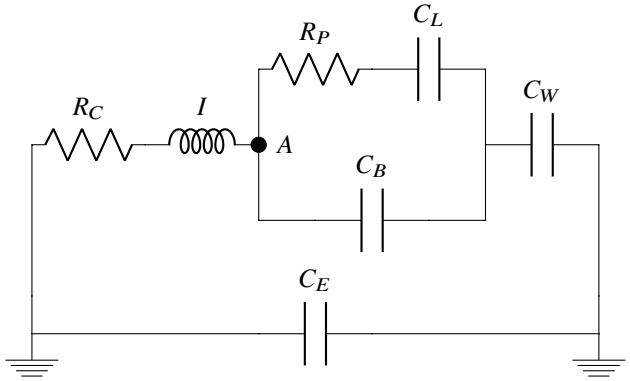

Fig. 7: The Mead model of respiratory mechanics. Ground potential corresponds to atmospheric pressure. The voltage between point A and ground represents intratracheal pressure. All components are described in Table III.

Oxygen delivery is modelled here by a constant pressure source applied to the narrow channels in the wall of the endotracheal tube (see Fig. 3). Valve switching and compression-decompression can affect oxygen insufflation pressure. A buffer tank in parallel with the oxygen source make these effects negligible. Therefore, the oxygen source is modelled as an ideal voltage source V_{in}. A resistor in series with V_{in} represents the resistance of the narrow channels with a value R_{BT}, calculated according to experimental pressures and flows from [8]. In the case of CIO, V_{in} is constant at a value equivalent to the pressure regulator setting of 2.5 bar. In PIIO, V_{in} is a square wave with a 50 % duty cycle and 600 ms period, and a voltage matching the pressure regulator setting of 4.5 bar. The values of R_{BT} and V_{in} used in the models are given in Table IV.

The compressions and decompressions from the mCPR device result in a change in pressure against the chest wall. They are therefore represented as a voltage source in series with the the lung capacitor C in the RIC model and the chest wall capacitor C_W in the Mead model. The voltage was varied in a trapezoidal waveform with 100 ms flanks representing the constant speed of the mCPR device's piston used in the preclinical experiment [8]. The waveform was given a 50 % duty cycle, 600 ms period, and 200 ms delay relative to the oxygen insufflation waveform. The decompression phase voltage was set to zero as the piston exerts no pressure on the chest wall. The voltage for the compression phase

TABLE IV: Square-wave oxygen insufflation pressure V_{in} and oxygen delivery tube resistance R_{BT} used in the models.

	V_{in} Pressure (kV)	R_{BT} (kΩ)
CIO	2.55	10.2
PIIO	4.59	12.0

was tuned such that the difference between the maximal and minimal intratracheal pressure during PIIO matched the value 15 cmH_2O observed in the preclinical study: 22.5 V for RIC and 16 V for Mead.

The complete models including oxygen insufflation and mCPR are shown in Fig. 8 and Fig. 9. They were implemented using OpenModelica [14]. The system representations in state space form are given by equations (1) and (2) for RIC and Mead, respectively, with oxygen insufflation and chest compression pressure as input u and intratracheal pressure as output y. State x_1 represents lung pressure and state x_2 represents central airway flow. In equation (2) states x_3 and x_4 represent chest wall and main bronchi pressure, respectively.

$$\begin{aligned}\dot{x} &= \begin{bmatrix} -\frac{1}{R_{BT}C} & \frac{1}{C} \\ -\frac{1}{I} & -\frac{R}{I} \end{bmatrix} x + \begin{bmatrix} \frac{1}{R_{BT}C} & -\frac{1}{R_{BT}C} \\ 0 & -\frac{1}{I} \end{bmatrix} u \\ y &= \begin{bmatrix} 1 & 0 \end{bmatrix} x + \begin{bmatrix} 0 & 1 \end{bmatrix} u \end{aligned} \tag{1}$$

$$\begin{aligned}\dot{x} &= \begin{bmatrix} -\frac{1}{R_P C_L} & 0 & 0 & \frac{1}{R_P C_L} \\ 0 & -\frac{R_C}{I} & -\frac{1}{I} & -\frac{1}{I} \\ 0 & \frac{1}{C_W} & -\frac{1}{R_{BT}C_W} & -\frac{1}{R_{BT}C_W} \\ \frac{1}{R_P C_B} & \frac{1}{C_B} & -\frac{1}{R_{BT}C_B} & -\frac{R_{BT}+R_P}{R_{BT}R_P C_B} \end{bmatrix} x \\ &+ \begin{bmatrix} 0 & 0 \\ 0 & -\frac{1}{I} \\ \frac{1}{R_{BT}C_w} & -\frac{1}{R_{BT}C_W} \\ \frac{1}{R_{BT}C_B} & -\frac{1}{R_{BT}C_B} \end{bmatrix} u \\ y &= \begin{bmatrix} 0 & 0 & 1 & 1 \end{bmatrix} x + \begin{bmatrix} 0 & 1 \end{bmatrix} u \end{aligned} \tag{2}$$

B. Experiment

The experimental data used here was published in [8], where the experimental protocol is described in detail. Twenty Swedish domestic pigs, 25–30 kg in weight, were used following the Utstein-style guidelines for CPR research

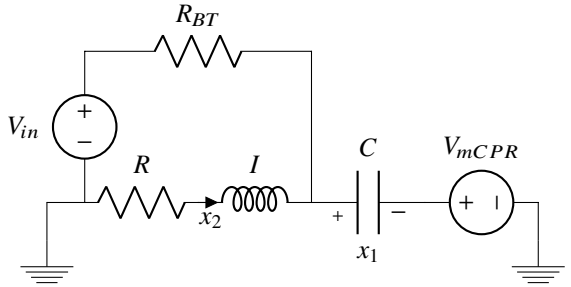

Fig. 8: Adapted RIC model of the experimental setup. Ground potential corresponds to atmospheric pressure. R_{BT} is the resistance of the narrow channels in the wall of the Boussignac endotracheal tube. V_{in} is oxygen insufflation pressure. V_{mCPR} is chest compression pressure. All other components are described in Table II. State x_1 is the voltage across C and x_2 is the current through I.

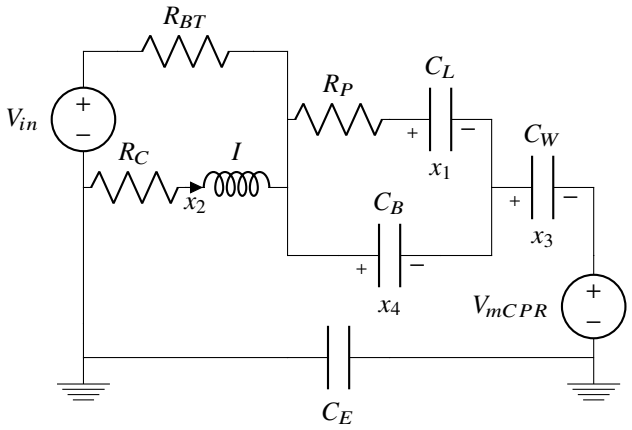

Fig. 9: Adapted Mead model of the experimental setup. Ground potential corresponds to atmospheric pressure. R_{BT} is the resistance of the narrow channels in the wall the Boussignac endotracheal tube. V_{in} is the oxygen insufflation pressure. V_{mCPR} is chest compression pressure. All other components are described in Table III. State x_2 is the current through I and states x_1, x_3, and x_4 are the voltages across C_L, C_W, and C_B, respectively.

[15]. The animals were stratified into two groups of 10 animals each. One group received CIO and the other PIIO. The study was run under ethics approval M174-15, issued by the "Malmö/Lunds regionala djurförsöketiska nämnd" (REB), and the animals received care in compliance with [16] guidelines.

Mechanical CPR was performed by a LUCAS device (first generation pneumatic version, Jolife AB, Lund, Sweden) at a 50 % duty cycle and 100 compressions per minute frequency.

Ventilation was administered through Boussignac endotracheal tube (Boussignac E.T. tube for cardiac arrest, VYGON, Ecouen, France). A pressure transducer (DTX Plus, Argon Medical Devices, Frisco, USA) was connected to two narrow channels in the wall of the Boussignac tube through air-filled plastic tubing with non-flexible walls to measure intratracheal pressure. The transducer signal was recorded by a data aquisition system described in [17]. Due to the low-pass filtering effect of air in the pressure measurement

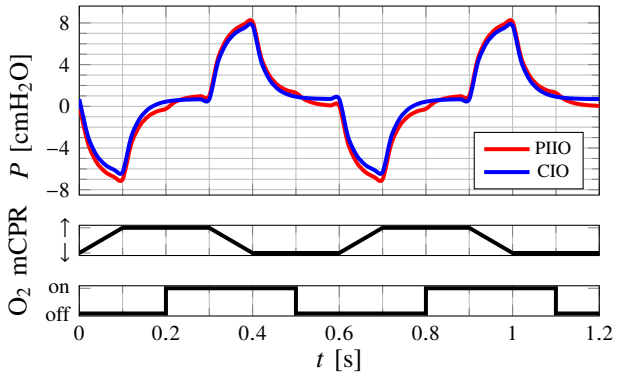

Fig. 10: PIIO and CIO intratracheal pressure responses P from RIC model simulations.

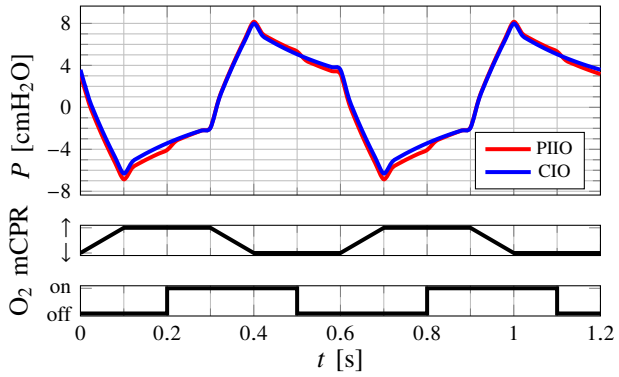

Fig. 11: PIIO and CIO intratracheal pressure responses P from Mead model simulations.

tubes in [8], time-averaged maximum, mean, and minimum intratracheal pressure are used for comparison rather than real-time P_{trachea}.

A Festo LRP-1 pressure regulator (Festo, Esslingen am Nackar, Germany) in series with a 605 ml buffer tank was used to provide a steady pressure oxygen source. During PIIO the pressure regulator was set to 4.5 bar resulting in 23 L/min oxygen flow through narrow channels in the wall of the Boussignac tube as measured by a Medimeter-30 rotameter (Mediline, Saint Helens, England). Under these conditions oxygen flow would cease if the intratracheal pressure exceeded 20 cmH_2O, giving ample margin to 50 cmH_2O where there is an increased risk of barotrauma [5]. CIO was delivered through the same type of endotracheal tube used during PIIO but with the the oxygen pressure set to 2.5 bar. This resulted in 15 L/min of oxygen flow, previously shown to provide sufficient ventilation and oxygenation[18]. The CIO setup is described in detail by Steen et al.[7].

Oxygen insufflation was switched using a Festo MHE4 direct valve (Festo, Esslingen am Nackar, Germany) with a switching time of 3.5 ms and nominal flow of 400 L/min. The valve and LUCAS device were coordinated according to Fig. 4 by a preprogrammed electronic controller.

III. Results

The simulated intratracheal pressure (P_{trachea}) responses shown in Fig. 10 and Fig. 11 capture qualitative differences in P_{trachea} between PIIO and CIO observed in the preclinical study [8]. In particular, both models show lower decompression phase minimal and mean P_{trachea} during PIIO compared to CIO. The difference between maximal and minimal P_{trachea} over a full compression-decompression cycle was also higher for PIIO in both models.

The experimental results in [8] show a 40 % lower minimal P_{trachea} and 25 % lower mean P_{trachea} during PIIO compared to CIO. The maximal P_{trachea} was the same during both methods, resulting in a 114 % higher difference between maximal and minimal P_{trachea} during PIIO compared to CIO. A comparison of the results from the simulations and experiment are given in Table V.

TABLE V: Percent change from CIO to PIIO for minimal, mean, and difference between maximal and minimal intratracheal pressure values P_{trachea}. $\Delta P_{\text{trachea}}$ represents the difference between minimal and maximal P_{trachea}.

	Relative change from CIO to PIIO		
	minimal P_{trachea}	mean P_{trachea}	$\Delta P_{\text{trachea}}$
Experiment	−40 %	−25 %	114 %
RIC	−11 %	−27 %	7 %
Mead	−9 %	−15 %	5 %

IV. Discussion

The RIC and Mead models capture qualitative differences between intratracheal pressure P_{trachea} during PIIO and CIO that were observed in the preclinical study: PIIO yields lower decompression phase mean and minimal P_{trachea} as well as a higher difference between maximal and minimal P_{trachea} over a full compression-decompression cycle. However, the differences are less pronounced in the simulations. As intended with PIIO, Fig. 10 and 11 show PIIO P_{trachea} rising compared to CIO during oxygen insufflation prior to compression from 0.2 s to 0.3 s. Conversely, PIIO P_{trachea} drops when insufflation is stopped prior to decompression from 0.5 s to 0.6 s.

In contrast to the RIC model, the Mead model does not reach steady state P_{trachea} during each compression and decompression phase, as seen from 0.1 s to 0.3 s (decompression) and 0.4 s to 0.6 s (compression) in Fig. 11. The RIC model simplifies compressions as being applied directly to the lungs, whereas they are applied to the chest wall C_W in the Mead model. Although the lung capacitor C_L and C_W are in series, lowering their total capacitance (a more compliant fluidic system), parameter fitting for the Mead model leads to abnormally high C_L values relative to RIC models, as noted in [12], [13], slowing the overall dynamics. In comparison, the contribution of the bronchial tree compliance C_B in parallel with C_L is negligible. However the peripheral resistance in series with C_L impedes charging and discharging of the capacitor, further slowing the system dynamics. These slow dynamics help account for the Mead model showing the smallest P_{trachea} difference between CIO and PIIO.

The preclinical study [8] focused on measuring CPP, and only captured time-averaged P_{trachea}. Further experimental evaluation of PIIO is planned wherein the hardware will be modified to enable fitting of the RIC and Mead parameters. Real-time signals will be used to identify the parameters and, if suggested by the data, adapt the model structures to arrive at a CPR simulation that is quantitatively correct. Currently, the models use P_{trachea} as an intermediate parameter for how variations in intrathoracic pressure effect the heart during CPR. The model of respiratory mechanics could be linked with a model of heart dynamics using aortic and right atrial pressure measurements. This would help clarify the relation between P_{trachea} and hemodynamics during CPR. The phase shift currently used in PIIO was found heuristically to optimize CPP. A more complete model would help to confirm this or suggest further improvements.

V. Conclusion

Common electronic circuit models of respiratory mechanics capture qualitative differences in intratracheal pressure during PIIO and CIO observed in preclinical experiments. Further model development and experimental data is required to make quantitative comparisons between the simulations and experimental results.

References

[1] S. Steen, Q. Liao, L. Pierre, A. Paskevicius, and T. Sjöberg, "Evaluation of lucas, a new device for automatic mechanical compression and active decompression resuscitation," *Resuscitation*, vol. 55, no. 3, pp. 285–299, 2002.

[2] N. A. Paradis, G. B. Martin, E. P. Rivers, M. G. Goetting, T. J. Appleton, M. Feingold, and R. M. Nowak, "Coronary perfusion pressure and the return of spontaneous circulation in human cardiopulmonary resuscitation," *Jama*, vol. 263, no. 8, pp. 1106–1113, 1990.

[3] M. Frenneaux and S. Steen, "Hemodynamics of cardiac arrest," in *Cardiac arrest: the science and practice of resuscitation medicine*, N. A. Paradis, H. R. Halperin, K. B. Kern, V. Wenzel, and D. A. Chamberlain, Eds., Cambridge University Press, 2007, ch. 17, pp. 347–366.

[4] M. T. Rudikoff, W. L. Maughan, M. Effron, P. Freund, and M. L. Weisfeldt, "Mechanisms of blood flow during cardiopulmonary resuscitation.," *Circulation*, vol. 61, no. 2, pp. 345–352, 1980.

[5] R. Haake, R. Schlichttg, D. R. Ulstad, and R. R. Henschen, "Barotrauma: Pathophysiology, risk factors, and prevention," *Chest*, vol. 91, no. 4, pp. 608–613, 1987.

[6] Q. Liao, T. Sjöberg, A. Paskevicius, B. Wohlfart, and S. Steen, "Manual versus mechanical cardiopulmonary resuscitation. an experimental study in pigs," *BMC cardiovascular disorders*, vol. 10, no. 1, p. 53, 2010.

[7] S. Steen, Q. Liao, L. Pierre, A. Paskevicius, and T. Sjöberg, "Continuous intratracheal insufflation of oxygen improves the efficacy of mechanical chest compression-active decompression cpr," *Resuscitation*, vol. 62, no. 2, pp. 219–227, 2004.

[8] K. Soltesz, H. Pigot, A. Paskevicius, L. Qiuming, T. Sjöberg, and S. Steen, "Phase-controlled intermittent intratracheal insufflation of oxygen during chest compression mCPR improves coronary perfusion pressure over continuous insufflation," *Resuscitation*, vol. 138, pp. 215–221, 2019.

[9] A. B. Otis, C. B. McKerrow, R. A. Bartlett, J. Mead, M. McIlroy, N. Selverstone, and E. Radford Jr, "Mechanical factors in distribution of pulmonary ventilation," *Journal of applied physiology*, vol. 8, no. 4, pp. 427–443, 1956.

[10] J. Mead, "Mechanical properties of lungs," *Physiological reviews*, vol. 41, no. 2, pp. 281–330, 1961.

[11] M. Schmidt, B. Foitzik, O. Hochmuth, and G. Schmalisch, "Computer simulation of the measured respiratory impedance in newborn infants and the effect of the measurement equipment," *Medical engineering & physics*, vol. 20, no. 3, pp. 220–228, 1998.

[12] B. Diong, H. Nazeran, P. Nava, and M. Goldman, "Modeling human respiratory impedance," *IEEE Engineering in Medicine and Biology Magazine*, vol. 26, no. 1, p. 48, 2007.

[13] S. Baswa, H. Nazeran, P. Nava, B. Diong, and M. Goldman, "Evaluation of respiratory system models based on parameter estimates from impulse oscillometry data," in *2005 IEEE Engineering in Medicine and Biology 27th Annual Conference*, IEEE, 2006, pp. 2958–2961.

[14] (2019). Openmodelica, [Online]. Available: `https://build.openmodelica.org/omc/builds/windows/releases/1.13/2/64bit/`.

[15] A. H. Idris, L. B. Becker, J. P. Ornato, J. R. Hedges, N. G. Bircher, N. C. Chandra, R. O. Cummins, W. Dick, U. Ebmeyer, H. R. Halperin, *et al.*, "Utstein-style guidelines for uniform reporting of laboratory cpr research," *Circulation*, vol. 94, no. 9, pp. 2324–2336, 1996.

[16] S. Louhimies, "Directive 86/609/eec on the protection of animals used for experimental and other scientific purposes," *Alternatives to Laboratory Animals*, vol. 30, no. 2_suppl, pp. 217–219, 2002.

[17] K. Soltesz, C. Sturk, A. Paskevicius, Q. Liao, G. Qin, T. Sjöberg, and S. Steen, "Closed-loop prevention of hypotension in the heartbeating brain-dead porcine model," *IEEE Transactions on Biomedical Engineering*, vol. 64, no. 6, pp. 1310–1317, 2016.

[18] K. B. Kern, J. R. Nelson, S. A. Norman, M. M. Milander, and R. W. Hilwig, "Oxygenation and ventilation during cardiopulmonary resuscitation utilizing continuous oxygen delivery via a modified pharyngeal-tracheal lumened airway," *Chest*, vol. 101, no. 2, pp. 522–529, 1992.

Acknowledgment

This project was financed by VINNOVA grant 2017-04667. The funding source has not influenced any aspect of the study or manuscript. The authors would like to thank Quiming Liao and Trygve Sjöberg of the Department of Cardiothoracic Surgery, Lund University and Skåne University Hospital, for their support and input.